JOURNAL OF CATALYSIS 155, 303–311 (1995)

FTIR Spectroscopy of Nitric Oxide Adsorption on Pd/Al_2O_3: Evidence of Metal–Support Interaction

T. E. Hoost,[1] K. Otto, and K. A. Laframboise

Ford Motor Company, Research Laboratory, MD 3179 SRL, P.O. Box 2053, Dearborn, Michigan 48121

Received August 8, 1994; revised February 27, 1995

Automotive three-way catalysts containing Pd as the only precious metal have certain advantages over current formulations consisting of various mixtures of Pt, Pd, and Rh. In this study, the adsorption of NO on 2 wt% Pd/Al_2O_3 was investigated using infrared spectroscopy. Bands for NO on Pd were assigned to linear (1753–1750 cm^{-1}), twofold bridged (1615–1599 cm^{-1}), and threefold bridged (1580–1572 cm^{-1}) adsorption modes. For Pd supported on alumina, linear NO was favored on the reduced catalyst while two- and threefold bridged NO were favored on the oxidized catalyst. Upon heating, a decrease in the linear form was accompanied by increases in the two- and threefold bridged forms up to the highest temperature measured (300°C). This result may indicate a conversion of the linear to bridged adsorption modes upon heating. NO adsorption on pure alumina revealed a band near 1807 cm^{-1} attributable to weak, linear adsorption. This band increased drastically upon oxidation of the Pd/Al_2O_3 catalyst, indicating enhanced NO adsorption on alumina due to the presence of palladium. Conventional spillover from Pd to alumina was ruled out. The increased intensity is explained by adsorption of NO on alumina sites involved in a metal–support interaction brought about by catalyst oxidation. NO adsorption on La-promoted Pd/Al_2O_3 was less than on the unpromoted catalyst. Possible explanations are an increase in NO dissociation and coverage of Pd by the modifier.

1. INTRODUCTION

Recently, there has been much interest in Pd-only catalysts as alternatives to traditional Pt- and Rh-containing three-way catalysts (TWCs). Several studies have demonstrated that when promoted by lanthana, Pd catalysts have similar hydrocarbon, CO, and NO_x removal activities under near-stoichiometric conditions compared to Rh-containing TWCs (1).

The primary objective of this work was to establish how metal-support interactions may affect the adsorption of NO on Pd/Al_2O_3 catalysts. Previous work (2) has shown the formation of a well-dispersed, oxygen- rich Pd/Al_2O_3 phase upon oxidation of catalysts of low metal concentration. A similar species was also observed by EXAFS (3). Based on a comparison with EXAFS results of base-metal aluminates (4, 5), Lesage-Rosenberg *et al.* (3) proposed that this dispersed species may have a structure close to that of an isolated Pd aluminate.

It may be expected that compared to base-metal aluminates, a metal–support interaction in Pd/Al_2O_3 would result in considerable NO uptakes because of the relatively high noble character of Pd. Yao and Shelef (6) studied NO adsorption on several base-metal aluminate spinels and compared area-specific NO uptakes to those on the corresponding oxides. Uptakes of NO by the aluminates were generally less than those on the corresponding oxides. However, the uptakes by the aluminates were greater than those measured on pure alumina. The extent of NO adsorption was suggested to depend on surface coordination of the base-metal ions and, consequently, on the degree of shielding from the surface by oxygen anions (6, 7). These studies confirmed that foreign metals with greater noble character tend to interact less strongly with alumina to form aluminates. This would result in less shielding from the surface and a corresponding increase in NO uptake.

The literature contains several vibrational studies of NO adsorption on Pd (8–17). These studies have established linear, bent, and bridged adsorption modes for NO on the metal. There have been no reports of dinitrosyl species on Pd surfaces. In the present study, properties of surface intermediates during NO adsorption on Pd/Al_2O_3 catalysts are further elucidated using Fourier-transform infrared spectroscopy (FTIRS). In particular, effects of the metal–support interaction on NO adsorption are studied. Effects of lanthana promotion on the NO adsorption on Pd/Al_2O_3 are briefly addressed, as well. We caution at the onset that while infrared spectroscopy is a useful means of studying adsorbed species, the technique allows only an indirect view of these species and their adsorption sites, and, consequently, band assignments tend to be provisional.

---

[1] To whom correspondence should be addressed. Fax: (313) 248-5627. E-Mail: thoost@smail.srl.ford.com.

0021-9517/95 $12.00

2. EXPERIMENTAL

2.1. *Catalyst Preparation and Characterization*

A sample containing 2 wt% Pd was prepared using defumed γ-Al_2O_3 (Degussa alumina C, 100 m^2/g, precalcined at 600°C for 16 h). The alumina support was immersed in an aqueous solution (pH $\approx$ 12.5) containing an appropriate amount of diammine palladium (II) nitrite (Strem, 5 wt% $Pd(NH_3)_2(NO_2)_2$) as the metal precursor. Water was gradually removed while the slurry was stirred in a beaker on a hot plate. The catalyst was finally calcined in static air at 600°C for 12 h. A second Pd/Al_2O_3 catalyst was promoted by lanthana. Using the incipient wetness technique, alumina was first impregnated with an aqueous solution of lanthanum nitrate to produce a sample of 10 wt% La_2O_3/Al_2O_3 which was precalcined at 800°C (18). Lanthana promotion decreased the BET surface area of the support from 104 to 90 m^2/g. The mixed support was then treated with the Pd solution as described for the preparation of the unpromoted Pd/Al_2O_3 catalyst. Hydrogen chemisorption measurements using the double-isotherm method of Benson *et al.* (19) established that the 2 wt% Pd/Al_2O_3 and 2 wt% Pd/(10 wt% La_2O_3/Al_2O_3) catalysts have apparent metal dispersions of 16 and 5%, respectively. The catalysts have BET surface areas of 99 and 91 m^2/g, respectively.

2.2. *Infrared Spectroscopy*

Adsorption experiments were performed in situ using a high-vacuum IR cell (base pressure of 5×10^{-8} Torr; 1 Torr = 133.3 Pa) equipped with CaF_2 windows. Catalyst powder samples were pressed into gold wire mesh at 138 bar. A chromel–alumel thermocouple was spot-welded to the center of the grid. The sample was fixed onto a transposable probe arm which also allowed resistive heating of the specimen. Spectra were recorded using a Mattson Cygnas 100 FTIR spectrometer multiplexed to a computer. All spectra were recorded as single background beam experiments and then ratioed with the initial, evacuated background spectrum. The spectral resolution was 4 cm^{-1}.

Research grade gases (O_2 99.998%, H_2 99.996%) from Matheson were used without further purification. NO (Matheson, 99.0%) was purified by trap-to-trap distillation (20). Depending on its thermodynamic state, the purified product was either a white solid, a light-blue liquid, or a colorless gas.

In situ catalyst pretreatment was as follows. For oxidation, the sample was evacuated at 400°C and treated at temperature in 100 Torr O_2 for 25 min. Finally, the sample was cooled to the adsorption temperature in 100 Torr O_2 and evacuated at temperature for 1 h. For reduction, the sample was evacuated at 400°C, treated in 100 Torr O_2 for 5 minutes, evacuated and reduced at 400°C in 100 Torr H_2 for 20 min. Finally, the samples were cooled to the adsorption temperature *in vacuo*. Adsorption of NO was performed between 25 and 300°C using pressures from 3 to 30 Torr.

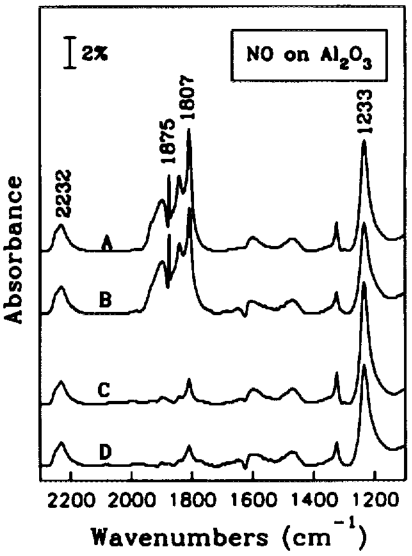

FIG. 1. NO adsorption on alumina at 25°C (A) Reduced, 30 Torr; (B) oxidized, 30 Torr; (C) reduced, evacuated; (D) oxidized, evacuated.

3. RESULTS

3.1. *NO on Alumina*

Spectra for NO adsorption at room temperature on reduced and calcined alumina, depicted in Fig. 1, were very similar. The slightly higher intensities for the reduced catalyst support do not appear to be significant. The features at 1845, 1875, and 1898 cm^{-1} are the *P*, *Q*, and *R* branches of gaseous NO. The infrared absorption band of gaseous N_2O occurs at 2224 cm^{-1} (21). The band of adsorbed N_2O exhibited a slight blue shift to 2232 cm^{-1} with respect to the free molecule. Bands below 1600 cm^{-1} have been reported for NO adsorption on alumina (8). They were attributable to nitrato complexes. These complexes are strongly adsorbed, as indicated by the moderate attenuation of the corresponding bands upon evacuation (Fig. 1). In fact, the absorption band at 1233 cm^{-1} continued to grow moderately, even after 1 h of evacuation. Figure 1 also displays a band at 1807 cm^{-1} for NO adsorption on alumina. Upon evacuation for 1 h, this band attenuated sharply, indicating that it is associated with weakly held NO. A spectrum obtained at 300°C and 30 Torr NO over neat alumina revealed complete removal of this peak at higher temperatures. Spectral band assignments can be refered to in Table 1.

TABLE 1

Infrared Band Assignments for Adsorbed Nitrogen Oxides on Pd/Al$_2$O$_3$ Catalysts

Band/cm^{-1}	Assignment
2232	NO$_2$ on alumina
1875	Gaseous NO; *P*, *Q*, *R* branches
1807	Linear NO weakly adsorbed on alumina. NO associated with Pd-alumina interaction.
1753–1750	Linear NO on Pd
1615–1599	Twofold bridged NO on Pd
1580–1572	Threefold bridged NO on Pd
1530	Not assigned
<1500	Nitrite and nitrate complexes associated with the support

3.2. NO on Supported Palladium

Figure 2 illustrates the infrared spectra for NO adsorption at room temperature on a reduced, 2 wt% Pd/Al$_2$O$_3$ catalyst. As expected, the spectral features are more pronounced at higher NO pressures. Wickham *et al.* (10) found no N$_2$O adsorption on Pd (111). This would suggest that the band at 2232 cm^{-1} (Fig. 2) is most likely due to N$_2$O adsorption on the alumina support (Fig. 1). As mentioned earlier, the frequency of adsorbed N$_2$O is significantly higher than that of gaseous N$_2$O.

Compared to NO adsorption on neat alumina (Fig. 1), there are two new absorption bands. The peak at 1753 cm^{-1} has been assigned to NO linearly adsorbed on Pd (nitrosonium ion) (9). At 1653 cm^{-1} there is a low-intensity feature, one of two bands which Moriki *et al.* (9) assigned to either negatively charged NO (the bent form) or bridged NO adsorbed on the metal in Pd/SiO$_2$. They observed the complement at 1575 cm^{-1}. However, from the spectra in Fig. 2, the latter band is not apparent on the alumina-supported catalyst at 25°C.

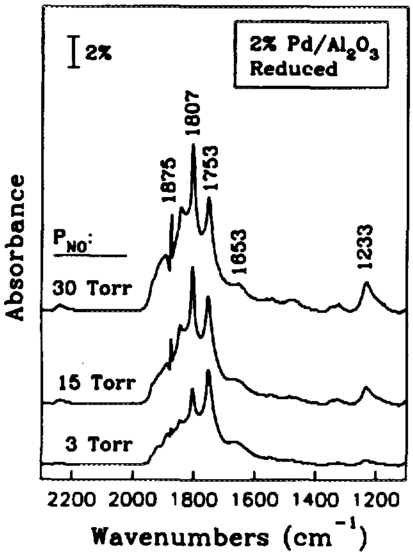

FIG. 2. Pressure dependence of NO adsorbed on reduced Pd/Al$_2$O$_3$ at 25°C.

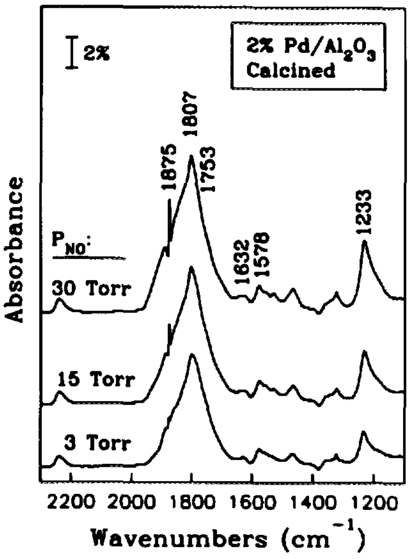

FIG. 3. Pressure dependence of adsorbed NO on oxidized Pd/Al$_2$O$_3$ at 25°C.

Work by Moriki *et al.* (9) on 5 wt% Pd/SiO$_2$ shows an attenuation of the peak associated with NO linearly adsorbed on an oxygen-covered catalyst when compared to the reduced form. For oxidized 2 wt% Pd/Al$_2$O$_3$, the dispersion would be higher compared to the silica-supported catalyst and the peak at 1753 cm^{-1} was not manifest at 25°C (Fig. 3). This suggests a more drastic decrease in the population of linearly adsorbed NO for catalysts with smaller metal particles. The peak at 1653 cm^{-1} is present at even lower intensity than observed for the reduced catalyst. This agrees with temperature-programmed desorption results of Moriki *et al.* (9) which showed that oxygen preadsorption on Pd decreased the ability of the metal to dissociate NO and increased the intensity of the NO desorption relative to the dissociation products. On an absolute scale, however, the amount of NO desorbed from the metal decreased with increasing oxygen coverage (9).

For the oxidized Pd catalysts, Fig. 3 shows that compared to the reduced Pd catalyst, the intensities of the bands below 1600 cm^{-1} increased slightly and the band at 1807 cm^{-1} increased considerably. Since peak intensities were similar for the reduced and calcined, neat alumina supports (Fig. 1), this indicates that oxidized Pd promotes adsorption of NO on the alumina support.

3.2.1. Sample evacuation at room temperature. Up-

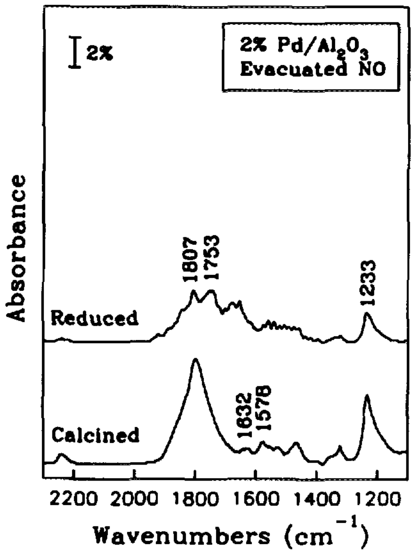

FIG. 4. Spectra after 1-h evacuation of NO on Pd/Al_2O_3 at 25°C.

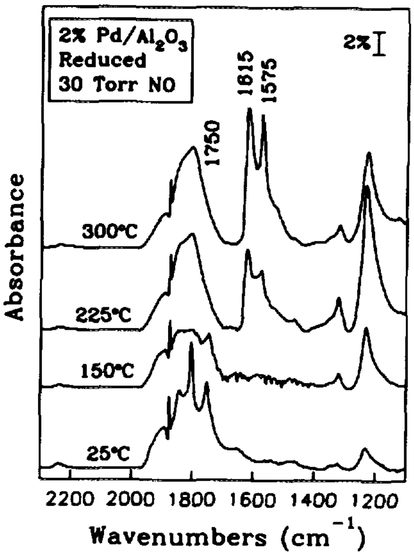

FIG. 5. Temperature effects on NO adsorbed on reduced Pd/Al_2O_3.

on evacuation, the spectral envelope associated with weakly held NO on the support of the reduced Pd catalyst behaved similarly as for the metal-free support (Figs. 1 and 4). The peak associated with the nitrosonium ion on reduced Pd decreased sharply while the band at 1653 cm^{-1} appears to have increased somewhat during the hour-long evacuation (Fig. 4).

For the oxidized catalyst, the linear adsorption mode for NO on Pd (1753 cm^{-1}) was absent after evacuation (Fig. 4). The bands at 1674 and 1575 cm^{-1} were of similar intensity as was observed before evacuation. Similar to what was observed before sample evacuation, the bands due to NO adsorption on the support were appreciably greater for the oxidized catalyst than for the reduced one after evacuation.

3.2.2. Temperature effects. Figure 5 displays spectra of NO adsorbed on reduced Pd/Al_2O_3 at different adsorption temperatures. The band at 1753 cm^{-1} associated with linearly adsorbed NO on Pd disappeared between 150 and 225°C. At 150°C, a band at about 1575 cm^{-1} appeared (9). Above 225°C, the peak at 1649 cm^{-1} shifted red and continued to intensify up to 300°C, the maximum adsorption temperature. Upon evacuation, the two associated species appeared to be quite stable at temperature as shown by the modest attenuation of the corresponding bands at 1577 and 1622 cm^{-1} (Fig. 6). Besides these bands, another feature appeared above 225°C at 1530 cm^{-1} which was not assigned.

In vacuum, the band at 1807 cm^{-1} associated with weakly held NO on the support of the reduced Pd/Al_2O_3 catalyst decreased considerably when the adsorption temperature was raised (Fig. 6). Other peaks associated with strongly held NO on the support due to nitrate formation (1320 and 1233 cm^{-1}) initially increased with temperature. However, even this strongly held NO began to decompose at higher temperatures, as shown by the spectrum obtained at 300°C (Fig. 6).

For oxidized Pd/Al_2O_3, the infrared spectra in Fig. 7 relate an increase in the bands near 1626 and 1575 cm^{-1} associated with NO on Pd when the adsorption temperature was increased. However, the growth of these features with temperature is much slower than was observed for

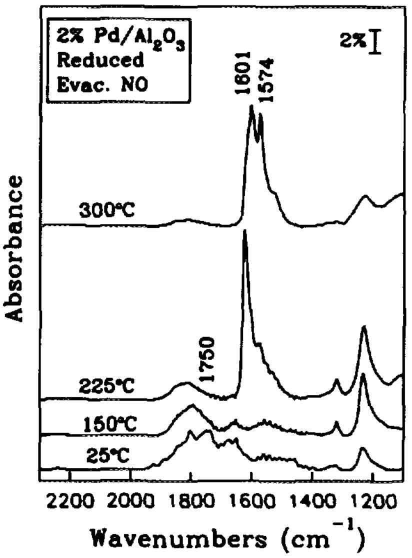

FIG. 6. Temperature effects on spectra after 1-h evacuation of NO on reduced Pd/Al_2O_3.

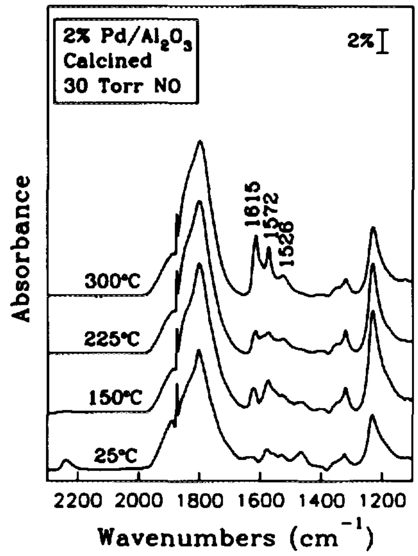

FIG. 7. Temperature effects on NO adsorbed on oxidized Pd/Al$_2$O$_3$.

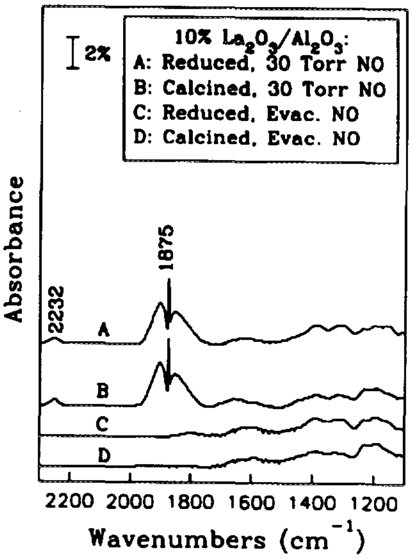

FIG. 9. NO adsorption on La-promoted alumina at 25°C.

reduced Pd/Al$_2$O$_3$ (Fig. 6). Remarkably, as shown in Figure 8, these two peaks continued to grow during the hour long evacuation (150 and 225°C). For the oxidized Pd/Al$_2$O$_3$ catalyst (Fig. 7), the 1807 cm^{-1} peak associated with NO on alumina grew modestly with adsorption temperature. Upon evacuation (Fig. 8), however, this peak decreased with temperature. As on the reduced catalyst, the peaks at 1321 and 1233 cm^{-1} associated with strongly held NO on the support initially increased with temperature. These peaks and the support peak at 1807 cm^{-1} (Fig. 8) were more stable *in vacuo* than the corresponding ones for the reduced catalyst (see Fig. 6).

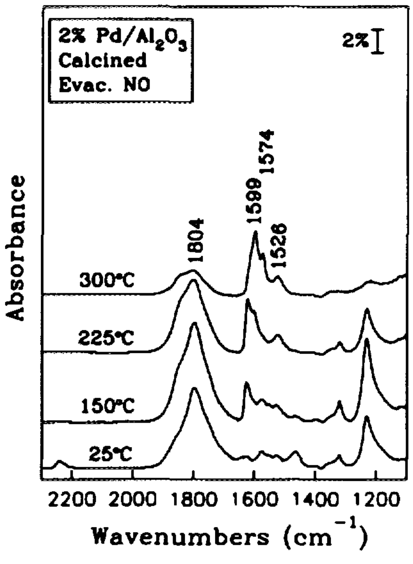

FIG. 8. Effect of temperature on spectra after 1-h evacuation of NO on oxidized Pd/Al$_2$O$_3$.

3.3. *La Modification*

3.3.1. NO on lanthana/alumina. The infrared spectra for the reduced and oxidized lanthana-modified alumina support were very similar (Fig. 9). Besides the peaks attributed to gaseous NO and adsorbed N$_2$O, Figs. 9*A* and 9*B* revealed only low features at 1640, 1391, and 1306 cm^{-1}. There were no counterparts for these features in the spectra for NO on neat alumina. Therefore, these low-frequency bands appear to be attributable to the interaction of NO with lanthana, possibly in the form of surface nitrato species. As depicted in Figures 9*C* and 9*D*, these features were quite stable upon evacuation at room temperature. In the spectra for the lanthana-modified alumina, all spectral features due to alumina were erased, except possibly for a very low-intensity band near 1231 cm^{-1}.

3.3.2. NO on lanthana-promoted palladium. The spectrum of NO on reduced, La-promoted Pd/Al$_2$O$_3$ exhibits a peak at 1753 cm^{-1}, corresponding to linearly adsorbed NO on Pd (Fig. 10*A*). The intensity of this peak was much less than was observed for reduced Pd/Al$_2$O$_3$ (Fig. 2). As with La-free Pd/Al$_2$O$_3$, this band was absent for the catalyst in the oxidized state (Fig. 10*B*). Upon evacuation, the spectrum (Fig. 10*C*) revealed bands at at 1674 and 1567 cm^{-1} on reduced, La-modified Pd/Al$_2$O$_3$. No features associated with NO adsorption on Pd could be distinguished for the oxidized catalyst either before or after evacuation (Figs. 10*B* and 10*D*).

Spectral comparison of evacuated La-promoted Pd/

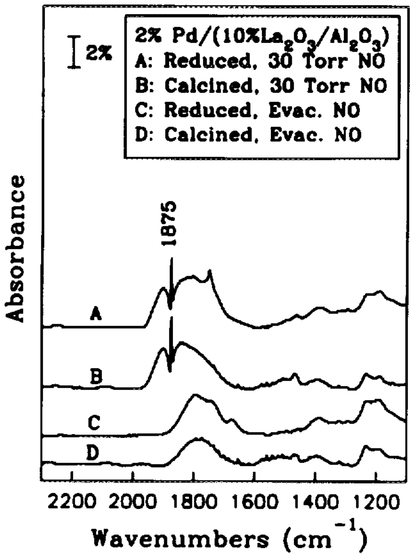

FIG. 10. NO adsorption on La-promoted Pd/Al_2O_3 at 25°C.

Al_2O_3 (Figs. 10*C* and 10*D*) and La-modified alumina (Figs. 9*C* and 9*D*), suggests that when Pd is present in the catalyst, alumina becomes more accessible for NO adsorption on the La-modified catalyst. Figure 10 exhibits an absorption band at 1807 cm^{-1}. This band which is associated with NO adsorption on alumina was not present for La-modified alumina without Pd. The intensities of bands below 1600 cm^{-1} associated with alumina remained very low on La-modified Pd/Al_2O_3. The low-frequency absorption bands associated with NO on lanthana (see Fig. 9) were still present, as well.

4. DISCUSSION

4.1. *Nitrosyl Species on Reduced Pd*

In the infrared spectra for NO adsorption on Pd/Al_2O_3, three absorption bands were attributed to NO interacting with the metal. Two of these bands (1753 and 1653 cm^{-1}) were manifest at room temperature while the third one (1577 cm^{-1}) became apparent only at higher temperature (Fig. 5). The frequency range for the internal stretching mode of atop-bonded NO is between 1650 and 2000 cm^{-1}. Wickham *et al.* (10) and Bertolo and Jacobi (11) reported EELS data which revealed energy losses for NO adsorption on Pd (111) at 1735 and 1745 cm^{-1}. These similar loss frequencies were assigned to the symmetric N–O stretch of atop-bonded NO. For NO on Pd (100), Nyberg and Uvdal (12) demonstrated that the corresponding loss occurred at somewhat lower energies (1675 cm^{-1}), and Jorgensen *et al.* (13) reported a shift in the loss frequency to 1720 cm^{-1} with increasing coverage. For high NO coverages on Pd/SiO_2, Grill and Gonzalez (14) and Moriki *et al.* (9) observed an infrared absorption band between 1753 and 1730 cm^{-1} which they assigned to linearly adsorbed NO. Thus, there are ample infrared spectroscopic and EELS data which indicate that for NO adsorbed on Pd/Al_2O_3, the absorption band at 1753 cm^{-1} may be assigned to the symmetric N–O stretch of linearly bonded NO.

For silica-supported Pd, Moriki *et al.* (9) suggested the existence of both a bent and bridged NO form. However, the two bands (1660–1650, 1580–1570 cm^{-1}) associated with these forms could not be specifically assigned. Work by Solomun (15) also indicates the difficulties involved with the assignment of bent nitrosyl species using infrared spectroscopy. In EELS studies (12), the distinction between these two modes of adsorption is often made by surveying the low-frequency region of the spectra for bending modes of the Pd–NO bond. However, these evaluations are not trivial. Although the NO stretching frequencies of the bent and bridged forms overlap (1525–1700 and 1480–1545 cm^{-1}, respectively), when both modes are present in the spectrum it has been generally accepted that the bridged form has its N–O stretch oscillating at lower frequency (15, 16). However, Chen and Goodman (22) demonstrated on Pd (111) that the stretching frequency of bent NO (1736 cm^{-1}) appears as a red shoulder to that of linear NO and is much higher than previously thought. Recent results by Goodman and coworkers (23) on Pd (100) and (111) suggest that assignment of the absorption bands at 1625 and 1575 cm^{-1} in Fig. 5 to NO adsorption on two- and threefold bridging sites, respectively, is more appropriate.

The temperature dependence of absorption bands associated with NO interacting with the metal has been summarized in Fig. 11. For reduced Pd/Al_2O_3, the amount of linear NO decreased with temperature whereas those of two- and threefold bridged NO increased (Fig. 11). Likewise, using EELS, Wickham *et al.* (10) showed that for saturation coverages of NO on Pd (111), atop and twofold bridged NO coexisted at −173°C. However, upon sample heating, the energy loss due to linear NO decreased sharply. At even higher temperatures (727°C), the loss due to bridged Pd also attenuated and eventually disappeared. Others reported comparable findings for the adsorption of NO on Pd (100) (12, 13) and Pd/SiO_2 (9).

4.2. *Nitrosyl Species on Oxidized Pd*

For oxidized Pd/Al_2O_3, the linear adsorption mode of NO was absent at prevailing temperatures (Fig. 7). At high temperatures, the two- and three-fold bridged forms developed more readily on the reduced Pd/Al_2O_3 catalyst than on the oxidized one (Fig. 11). The low-temperature spectra of the oxidized Pd/Al_2O_3 catalysts are somewhat similar to the high-temperature ones of the reduced samples. This raises the possibility that with increasing tem-

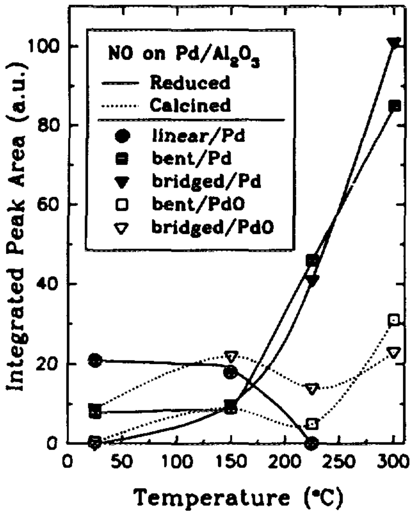

FIG. 11. Temperature dependence of surface nitrosyl species on reduced and oxidized Pd/Al$_2$O$_3$ at 30 Torr NO.

perature there may be a conversion of linear to bridged NO. If in addition to molecular desorption of linear NO from reduced Pd there is also a partial dissociation of the NO on dispersed Pd (24, 25), then the catalyst would be gradually oxidized by the oxygen left on the catalyst surface. Thus, at higher temperatures, increased NO dissociation would effectively turn a reduced Pd/Al$_2$O$_3$ catalyst into more oxidized one.

Nyberg and Uvdal (17) studied the effect of oxygen preadsorption for NO on Pd (100). Oxygen preferentially adsorbed in the hollow positions and adsorption of NO on atop sites was more favorable on the oxygen-covered surface than on the oxygen-free one, contrary to the present results. Linear sites were also reported to be favored for NO adsorption on oxygen-precovered Pt (111) (26), Rh (111) (27), and Ni (111) (28). For NO adsorbed on Pd/SiO$_2$, the three nitrosyl species behaved similarly on an oxygen-pretreated surface as on a clean one (9).

For alumina-supported Pd, the effect of preoxidation on the adsorption of NO can be compared to sulfur poisoning of NO adsorption on Pd (100) (13). Jorgensen *et al.* (13) reported a sharp attenuation of the electron energy loss due to the atop-bonded nitrosyl when the sulfur coverage was increased. As this happened, the EELS feature associated with bridge-bonded NO intensified with sulfur coverage. Sulfur poisoning was limited to simple site blocking, and LEED located the sulfur atoms in the fourfold hollows. In these locations, sulfur initially blocks adsorption in the atop site while the twofold bridging sites are significantly hindered only at higher sulfur coverage. Even so, there was still some NO adsorption observed in the twofold sites after saturation of the sulfur adlayer. A similar situation may occur on oxidized Pd/Al$_2$O$_3$. Thorough calcination to PdO may result in similar steric hindrances of NO adsorption sites on Pd, particularly since the atomic radius of oxygen is only slightly smaller than that of sulfur (29).

4.3. Support Effects

For NO adsorption on alumina, Solymosi and Rasko (8) observed several absorption bands below 1600 cm^{-1} which can be attributed to the formation of nitrato complexes. Besides these bands, Fig. 1 also manifests a band at 1807 cm^{-1} which attenuated sharply upon evacuation. Magnetic susceptibility studies of NO adsorption on alumina indicated that a rapid physical adsorption was followed by a slow chemisorption step (30, 31). Since the 1807 cm^{-1} band appears in the frequency range of linearly adsorbed NO (1650–2000 cm^{-1}), it is attributable to linear NO weakly held on the alumina surface. It should be noted that we did not find previous reports for stretching frequencies at 1807 cm^{-1} upon NO adsorption on alumina or Pd.

On reduced Pd/Al$_2$O$_3$, the intensity of the band at 1807 cm^{-1} (Fig. 2) was similar to that observed for neat alumina (Fig. 1). For oxidized Pd/Al$_2$O$_3$, the band intensified considerably (Fig. 3). This increase in the band at 1807 cm^{-1} is most likely due to NO adsorption on support sites that strongly interact with Pd, particularly under oxidizing conditions. EXAFS results of Lesage-Rosenberg *et al.* (3) have revealed that for well-dispersed Pd/Al$_2$O$_3$ catalysts, the fixation of the Pd cation involved octahedral aluminum-vacant sites of the support, forming locally a phase close to an aluminate. TPO work (2) also supports the formation of such a highly dispersed, oxygen-rich Pd/Al$_2$O$_3$ species upon catalyst oxidation. As indicated by the current FTIR results (cf. Figs. 2 and 3), this metal–support interaction may be responsible for the increase in the weakly held NO adsorbed on the support. Work by Yao and Shelef (6) on the adsorption of NO on bulk aluminate spinels showed that for foreign atoms such as Co, Ni, and Cu, the area-specific NO uptake increased by several orders of magnitude compared to the NO uptake measured on γ-alumina. The area-specific NO adsorption was greater for foreign metal atoms of higher nobility.

It is not altogether clear how the metal–support interaction in oxidized Pd/Al$_2$O$_3$ may accommodate NO adsorption. Using low-energy ion scattering spectroscopy (LEISS) on aluminate powders, Shelef *et al.* (7) demonstrated that a higher nobility of the foreign metal atom led to an increased tendency of this atom to be exposed at the spinel surface, thus increasing its accessibility to NO from the gas phase. Fu *et al.* (32) reported a red shift of 26 cm^{-1} for NO adsorbed on Cu^{2+} in CuAl$_2$O$_4$ with respect to the band observed for CuO. However, for the metal–support interaction in oxidized Pd/Al_2O_3, our FTIR results indicate an increase in the support band at 1807 cm^{-1} (cf. Figs. 2 and 3). In addition, for the oxidized catalyst, NO did not adsorb linearly on Pd (Figs. 3 and 7). It should be noted that previous reports on NO adsorption on oxidized Pd (100) (17) and oxidized Pd/SiO_2 (9) did not reveal N–O stretching frequencies near 1807 cm^{-1}. Thus, our observations suggest that NO did not adsorb on the metal but rather on the support moiety of the Pd–alumina interaction.

The aforementioned view of the metal–support interaction on oxidized Pd/Al_2O_3 agrees with the FTIR data because it predicts a limited amount of additional NO adsorption localized on the support around the site of the metal–support interaction. Since the additional NO adsorption appears to be localized, it does not seem likely that a relative increase in associative adsorption of NO on dispersed palladium oxide may bring about NO spillover onto the alumina support because such conventional spillover would require full participation of the support surface. From work function studies it is well-known that preadsorbed oxygen effectively removes charge from the metal surface (33). As predicted by Blyholder's model (34), this decrease in electrons from the surface strengthens the N–O bond due to decreased back-donation into the antibonding π^* orbital of the NO molecule. This would ostensibly result in a more associatively adsorbed NO, bound less tightly on Pd.

Thus, in principle, it is possible that this more weakly held NO would spill over more easily onto the alumina support. However, as mentioned before, the relatively modest increase in the band at 1807 cm^{-1} (cf. Figs. 2 and 3) does not support such widespread participation of the support. Moreover, upon evacuation of NO from reduced Pd/Al_2O_3, the band at 1807 cm^{-1} decreased sharply at all temperatures measured (Figs. 5 and 6). The slight intensity of the band at 1807 cm^{-1} remaining after sample evacuation is due to either NO adsorbed directly on the support, or NO associated with the metal–support interaction, perhaps enhanced by dissociated oxygen. The latter possibility would be favored at higher temperatures because, as mentioned before, no NO adsorption was measured on neat alumina at 300°C, whereas a slight, broad peak was observed for reduced Pd/Al_2O_3 at 300°C (Fig. 6). If the increase in the intensity of the band at 1807 cm^{-1} for oxidized Pd/Al_2O_3 would be due to conventional NO spillover, one would expect that since NO associated with the alumina surface of the reduced Pd/Al_2O_3 catalyst was easily evacuated, evacuation of the oxidized catalyst should decrease the band at 1807 cm^{-1} to the same intensity as for the band of the evacuated, reduced sample. Instead, the decrease in the intensity of the band at 1807 cm^{-1} for oxidized Pd/Al_2O_3 (Fig. 8) was far more modest than what was observed for reduced Pd/Al_2O_3 (Fig. 6).

One way to account for the greater amount of NO left at 1807 cm^{-1} after evacuation of the oxidized catalyst (compared to the reduced one) would be if catalyst oxidation would have changed the alumina support in such a way that additional anchoring sites for NO adsorption would be created. However, background TPO spectra of the same alumina support (2) confirmed it to be stable upon treatment in oxygen up to at least 800°C. A comparison of NO adsorption on alumina alternatively treated in hydrogen and oxygen (Fig. 1) also does not suggest any changes in the support that may lead to the formation of more NO adsorption sites on the support upon sample oxidation. It is therefore concluded that conventional spillover of NO with widespread participation of the support surface of the oxidized Pd/Al_2O_3 catalyst can be ruled out.

The support of the La-promoted catalysts contained 10 wt% lanthana. A comparison of FTIR spectra for NO on La-promoted and neat alumina (Figs. 9 and 1, respectively) indicates that absorption bands due to NO adsorption on the support were either entirely removed or greatly attenuated in the presence of the modifier. Bettman *et al.* (18) reported a sudden decrease in the slope for specific CO_2 adsorption as a function of lanthana concentration at 10.5 wt% La_2O_3/Al_2O_3 for materials synthesized using a similar procedure as our own. This change was attributed to an abrupt change in lanthana morphology from a dispersed, two-dimensional overlayer to a more crystalline phase due to excess lanthana at higher concentrations of the modifier. Similarly, based on point of zero charge and BET measurements, Subramanian *et al.* (35) estimated the transition point for the lanthana overlayer to be between 8 and 11 wt% La_2O_3/Al_2O_3 for supports also prepared like ours. Thus, for the La-promoted support, the drastic attenuation in the bands due to NO adsorption on alumina appears to be due to extensive coverage of the alumina surface by the modifier (Fig. 9).

La sharply attenuated NO adsorption on both reduced and oxidized Pd (Fig. 10). This attenuation is at least in part due to coverage of the metal by the modifier. Studies on lanthana-supported Pd and lanthana-promoted Pd/SiO_2 have indicated the ability of lanthana to partially cover Pd particles (36, 37). XRD results of Muraki *et al.* (38) indicated similar metal particle sizes for unpromoted and lanthana-promoted Pd/α-Al_2O_3 catalysts. Thus, although the Pd precursor was added to the catalyst after the modifier, it is quite reasonable that at the prevailing lanthana concentration the modifier would be able to effectively cover part of the Pd particles, resulting in the observed decrease in the apparent metal dispersion from 16 to 5%. Even so, a concurrent decrease in NO adsorption due to an increase in NO dissociation upon La promotion cannot be excluded. It has been demonstrated using XPS and LEISS that while room-temperature NO adsorption on alumina-supported Pd appears to be nondissociative, there is evidence of partly dissociative adsorption on lanthana-supported Pd (39, 40).

5. CONCLUSIONS

Infrared bands for NO adsorption on Pd in Pd/Al_2O_3 were attributed to linear (1753–1750 cm^{-1}), twofold bridged (1632–1599 cm^{-1}), and threefold bridged (1580–1572 cm^{-1}) forms of NO. Upon heating, a decrease in the linear form was accompanied by increases in the two- and threefold bridged forms up to 300°C, the highest temperature measured. This would suggest a conversion of the linear to the bridged adsorption modes upon heating. Contrary to previous EELS results for Pd single-crystal surfaces, preadsorbed oxygen on alumina-supported Pd decreased the amount of linear NO but increased the amounts of two- and threefold bridged NO. NO adsorption on alumina revealed a band near 1807 cm^{-1} which is attributed to weakly adsorbed, linear NO. This band increased dramatically upon oxidation of the Pd/Al_2O_3 catalyst, indicating participation of the support in the adsorption of NO due to the presence of the metal. Conventional spillover of NO with widespread participation of the alumina support could be ruled out. The increase in the support band was most likely due to adsorption of NO on alumina sites involved in a metal–support interaction brought about by catalyst oxidation. Associative NO adsorption on La-promoted Pd/Al_2O_3 was less than on the La-free catalyst, possibly due to an increase in NO dissociation and coverage by the modifier.

ACKNOWLEDGMENTS

We thank A. D. Logan, R. O. Carter, and W. G. Rothschild for their help with the FTIR instrument. We also thank R. W. McCabe, M. Shelef, and R. O. Carter for their helpful comments on the manuscript.

REFERENCES

1. Muraki, H., SAE Paper 910842 (1991).
2. Hoost, T. E., and Otto, K., *Appl. Catal. A* **92,** 39 (1992).
3. Lesage-Rosenberg, E., Vlaic, G., Dexpert, H., Lagarde, P., and Freund, E., *Appl. Catal.* **22,** 211 (1986).
4. Derouane, E. G., Simoens, A. J., and Vedrine, J. C., *Chem. Phys. Lett.* **52,** 549 (1977).
5. Greegor, R. B., Lytle, F. W., Chin, R. L., and Hercules, D. M., *J. Phys. Chem.* **85,** 1232 (1981).
6. Yao, H. C., and Shelef, M., in "The Catalytic Chemistry of Nitrogen Oxides," (R. L. Klimisch, and J. G. Larson, Eds.), p. 45. Plenum, New York, NY, 1975.
7. Shelef, M., Wheeler, M. A. Z., and Yao, H. C., *Surf. Sci.* **47,** 697 (1975).
8. Solymosi, F., and Rasko, J., *J. Catal.* **62,** 253 (1980).
9. Moriki, S., Inoue, Y., Miyazaki, E., and Yasumori, I., *J. Chem. Soc. Faraday Trans. I* **78,** 171 (1982).
10. Wickham, D. T., Banse, B. A., and Koel, B. E., *Surf. Sci.* **243,** 83 (1991).
11. Bertolo, M., and Jacobi, K., *Surf. Sci.* **226,** 207 (1990).
12. Nyberg, C., and Uvdal, P., *Surf. Sci.* **204,** 517 (1988).
13. Jorgensen, S. W., Canning, N. D. S., and Madix, R. J., *Surf. Sci.* **179,** 322 (1987).
14. Grill, C. M., and Gonzalez, R. D., *J. Phys. Chem.* **84,** 878 (1980).
15. Solomun, T., *J. Electroanal. Chem.* **199,** 443 (1986).
16. Raval, R., Blyholder, G., Haq, S., and King, D. A., *J. Phys. Condens. Matter* **1,** SB165 (1989).
17. Nyberg, C., and Uvdal, P., *Surf. Sci.* **256,** 42 (1991).
18. Bettman, M., Chase, R. E., Otto, K., and Weber, W. H., *J. Catal.* **117,** 447 (1989).
19. Benson, J. E., Hwang, H. S., and Boudart, M., *J. Catal.* **30,** 146 (1973).
20. Otto, K., and Shelef, M., *J. Catal.* **18,** 184 (1970).
21. London, J. W., and Bell, A. T., *J. Catal.* **31,** 32 (1973).
22. Chen, P. J., and Goodman, D. W., *Surf. Sci.* **297,** L93 (1993).
23. Xu, X., Chen, P., and Goodman, D. W., *J. Phys. Chem.* **98,** 9242 (1994).
24. Sugai, S., Watanabe, H., Miki, H., Kioka, T., and Kawasaki, K., *Vacuum* **41,** 90 (1990).
25. Sugai, S., Watanabe, H., Kioka, T., Miki, H., and Kawasaki, K., *Surf. Sci.* **259,** 109 (1991).
26. Bartram, M. E., Koel, B. E., and Carter, E. A., *Surf. Sci.* **219,** 467 (1989).
27. Root, T. W., Fisher, G. B., and Schmidt, L. D., *J. Chem. Phys.* **85,** 4679 (1986).
28. Erley, W., *Surf. Sci.* **205,** L771 (1988).
29. Weast, R. C. (Ed.), "CRC Handbook of Chemistry and Physics." CRC Press, Boca Raton, FL, 1982.
30. Solbakken, A., and Reyerson, L. H., *J. Phys. Chem.* **64,** 1903 (1960).
31. Solbakken, A., and Reyerson, L. H., *J. Phys. Chem.* **66,** 365 (1962).
32. Fu, Y., Tian, Y., and Lin, P., *J. Catal.* **132,** 85 (1991).
33. Ertl, G., and Koch, J., in "Adsorption–Desorption Phenomena," (F. Ricca, Ed.), p. 345. Academic Press, New York, 1972.
34. Blyholder, G., *J. Phys. Chem.* **68,** 2772 (1964).
35. Subramanian, S., Chattha, M. S., and Peters, C. R., *J. Mol. Catal.* **69,** 235 (1991).
36. Hicks, R. F., Yen, Q. J., and Bell, A. T., *J. Catal.* **89,** 498 (1984).
37. Rieck, J. S., and Bell, A. T., *J. Catal.* **99,** 278 (1986).
38. Muraki, H., Shinjoh, H., and Fujitani, Y., *Appl. Catal.* **22,** 325 (1986).
39. Graham, G. W., *Surf. Sci.* **268,** 25 (1992).
40. Logan, A. D., and Graham, G. W., *Surf. Sci.* **277,** L47 (1992).